

Novel 3-D interpenetrated Metal-Organometallic Networks based on self-assembly Zn(II)/Cu(II) from 1,1'-ferrocenedicarboxylic acid and 4,4'-bypiridine

María L. Ospina-Castro,^{a,b} Andreas Reiber,^b Gilberto Jorge,^c Edward E. Ávila,^a and Alexander Briceño^{a*}

^a *Laboratorio de Síntesis y Caracterización de Nuevos Materiales, Centro de Química, Instituto Venezolano de Investigaciones Científicas, San Antonio de Los Altos, Miranda, Venezuela. Fax: +58 212 5041320; Tel: +58 212 5041609; E-mail: abriceno@ivic.gob.ve*

^b *Laboratorio de la Interfase Inorgánica-Orgánica, Universidad de los Andes, Bogotá, Colombia.*

^c *Laboratorio de Electroquímica, Universidad Central de Venezuela, Caracas, Venezuela.*

^d *Programa de Ingeniería Ambiental, Universidad ECCI, Bogotá, Colombia.*

Electronic Supplementary Information Content:

1	General information and materials	3
2	Synthesis of compound 1.....	3
3	Synthesis of compound 2.....	3
4	FT-IR Measurement	3
5	Crystal structure determination.....	3
6	Differential pulse voltammetry.....	3
7	TGA-Measurement	3

Table S1. Experimental details for X-ray diffraction collected data and structural refinement.3

Table S2. Selected bond distances, angles, and torsion angle for compounds 1 and 2.3

Table S3. Hydrogen-bond geometry (Å, °) for compounds **1** and **2**.3

Fig. S1. Powder patterns for compounds 1 and 2 experimental (exp.) and calculated (calc.). Furthermore, the calculated powder diffraction patterns of starting ligands 4,4'-bpy (4,4'-bipyridil) and Fc (1,1'-ferrocenedicarboxylic acid) were included.....4

Fig. S2. Jahn-Teller effect in compounds 1 and 2. Comparative representation of coordination spheres surrounded of metallic ion, Zn (II)/Cu (II), it displayed some bond distances selected.....5

Fig. S3. FT-IR spectra for compound 1

Fig. S4. FT-IR spectra for compound 2

Fig. S5. TGA curves for compound 1 and 2.9

Fig. S6. Adsorption isotherms for N₂ (77 K). Red and blue line continued represent adsorption and desorption, respectively. (a) and (b) represent adsorption isotherms saturation pressure (P₀) equals 760 Torr for N₂ at 77 K9

Fig. S7. Differential pulse voltammograms showing graphs for compounds 1, 2 and 1,1'-ferrocenedicarboxylic acid, dissolved at a concentration of 1.0x10⁻³ M in DMF 0.1 M). The voltammograms were carried out at a scanning rate of 20 mVs⁻¹ (vs. Ag/AgCl).10

1 General information and materials.

All chemicals were commercially available and were purchased from Sigma-Aldrich as reagent grade quality and used without further purification. Elemental analysis was carried out on an EA1108 CHNS-O Fision Instrument.

2 Synthesis of compound 1.

1,1'-ferrocenedicarboxylic acid (50.1 mg, 0.11 mmol) and 4,4'-bipy (52.1 mg, 0.33 mmol) were mixed with H₂O and Zn(OAc)₂·2H₂O (73.3 mg, 0.33 mmol) and heated in a Teflon lined autoclave at 100 °C for three days. Good quality orange crystals were obtained. Yield: 25.2 % (26.5 mg). Anal. Calc. for {[Zn(4,4'-bipy)₂(₂OCFcCO₂)₂]}_n: C, 51.65 %; H, 3.55 %; N, 5.48 %. Found: C, 51.69 %; H, 3.60 %; N, 5.49 %. IR (cm⁻¹, KBr): 3517.61 (vs), 1573.34 and 1379.07 (m), 777 to 995 (w), 487 and 500 (m).

3 Synthesis of compound 2.

1,1'-ferrocenedicarboxylic acid (55.1 mg, 0.2 mmol) and 4,4'-bipy (33.5 mg, 0.2 mmol) were mixed with H₂O and Cu(OAc)₂·H₂O (20.4 mg, 0.1 mmol) and heated in a Teflon lined autoclave at 100 °C for three days. Good quality orange crystals were obtained. Yield: 30.3% (26.5 mg). Anal. Calc. for {[Cu(4,4'-bipy)₂(₂OCFcCO₂)₂]}·H₂O}n : C, 51.43%; H, 4.32%; N,5.45%. Found: C, 51.40%; H, 4.29%; N, 5.37%. IR (cm⁻¹, KBr): 3517.61 (vs), 1573.34 and 1379.07 (m), 777 to 995 (w), 487 to 500 (m).

4 Powder diffraction patterns data.

The powder diffraction data for compound **1** were collected with the high-resolution powder X-ray diffractometer Bragg-Brentano geometry on Panalitical, Empyrean S2 at University of ECCI, Cundinamarca-Colombia, with the powdered samples were mounted on the axis of the diffractometer and spun during measurements. Data were collected for several minutes with Co anode focus length and fine, powered at 40 kV-30 mA, divergence, anti-dispersive, Söller, detector slits 1 mm, 8 mm, 2.5° and 3 mm, respectively. Reflection's Bragg were detected with Pixel 3D™ 2x2 and into steps of 0.02° 2θ. And powder diffraction data for compound **2** were collected on an X-ray diffractometer Bragg-Brentano geometry Siemens, D5005 at Laboratory of Crystallography, Faculty of Science, University of The Andes, Mérida-Venezuela. These data were collected for several minutes with Cu K_α, powered at 40 kV-30 mA.

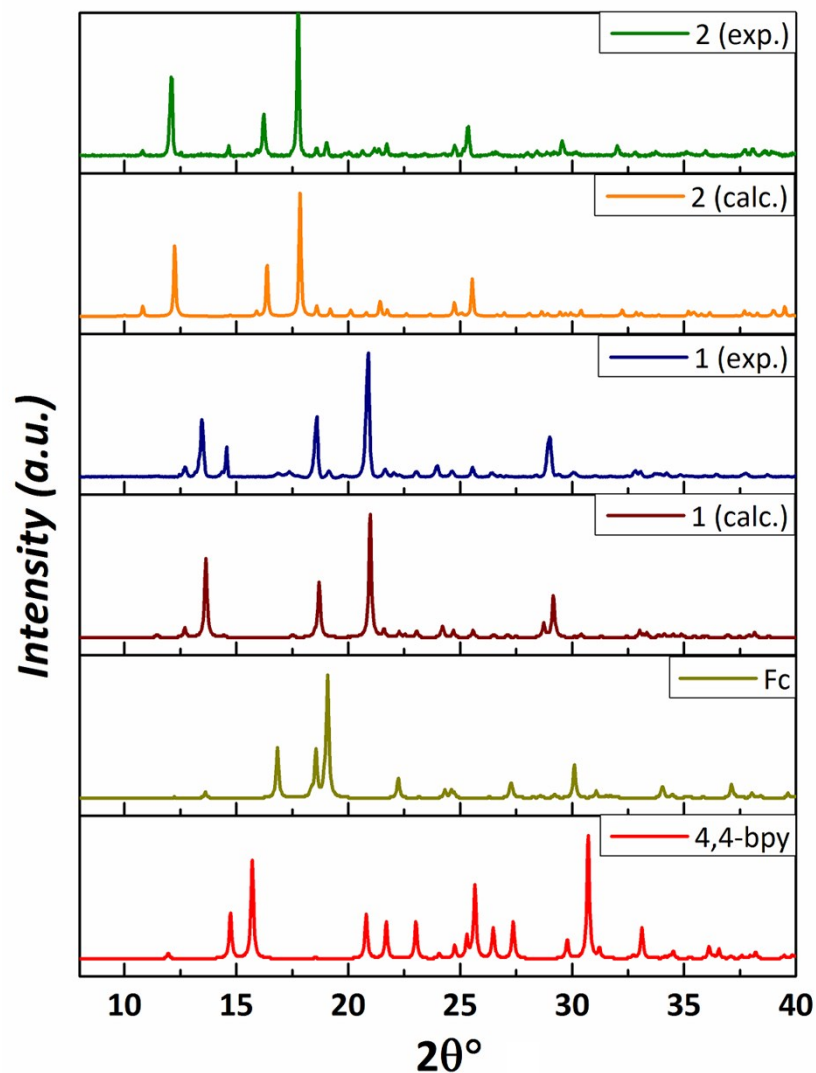


Fig. S1. Powder patterns for compounds **1** and **2** experimental (exp.) and calculated (calc.). Furthermore, the powder diffraction patterns include of the starting ligands 4,4'-bpy (4,4'-bipyridil) and Fc (1,1'-ferrocenedicarboxylic acid). Between the patterns of compound **1** and **2** there is a small displacement of the diffraction maxima because the data of compound **1** was taken and simulated considering Co K_{α} instead for compound **2** this was done with Cu K_{α} , respectively.

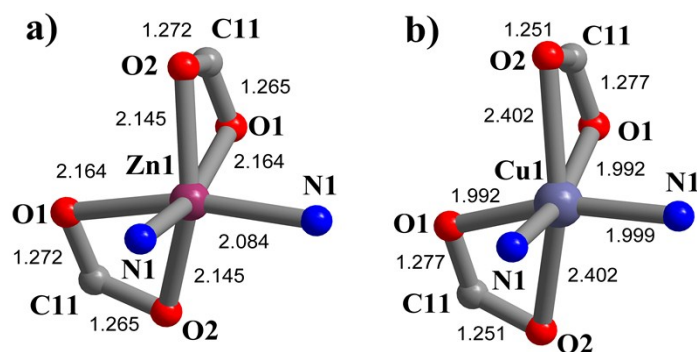


Fig. S2. Jahn-Teller effect in compounds **1** and **2**. Comparative representation of coordination spheres surrounded of metallic ion, Zn (II)/Cu (II), it displayed some bond distances selected.

5 FT-IR Measurement.

KBr pellets of the product compounds were used for IR data recording on a NICOLET MAGNA 560 spectrophotometer in the 400-4000 cm^{-1} region.

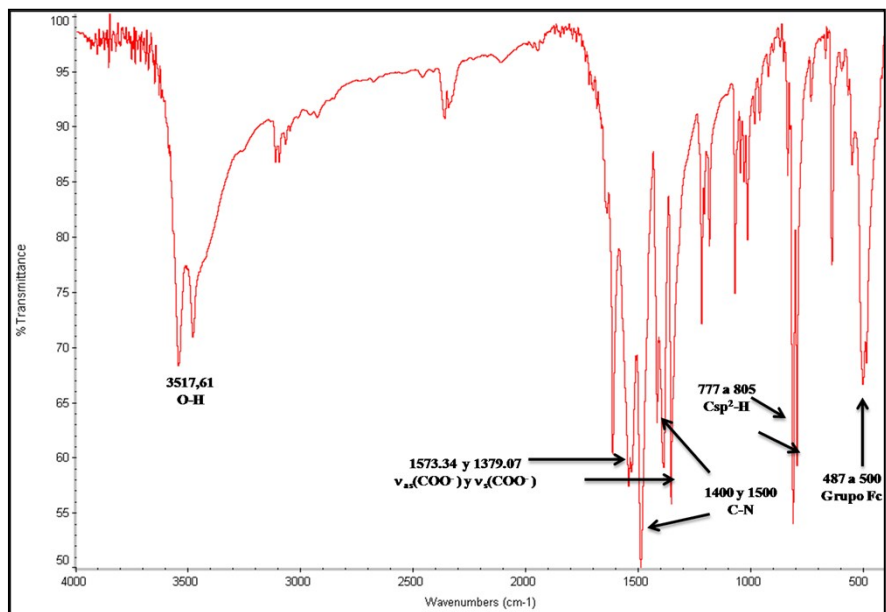


Fig. S3. FT-IR spectra for compound 1

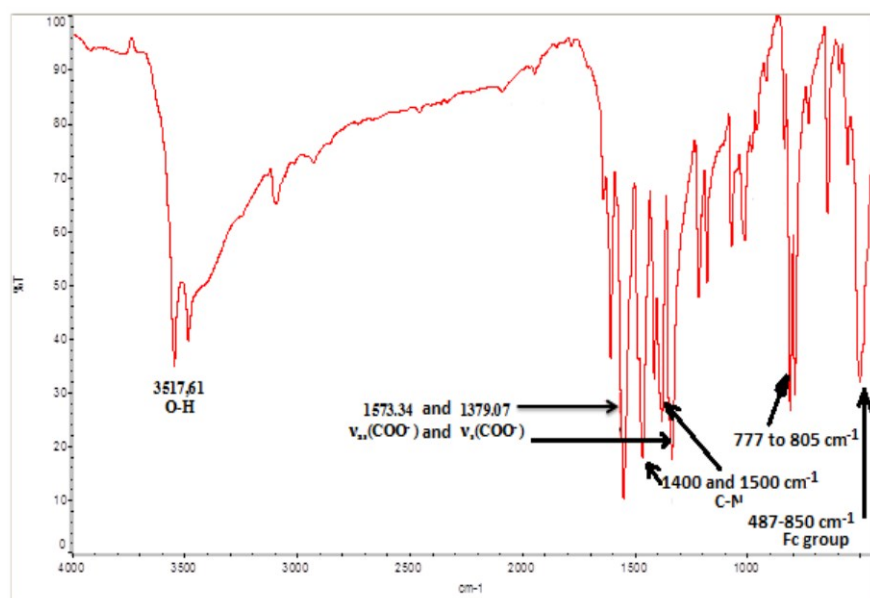


Fig. S4. FT-IR spectra for compound 2

6 Crystal structure determination.

All crystal structure measurements were carried out on an Agilent SuperNova, CrysAlis Pro, Oxford Cryojet, detector Atlas with Mo/Cu radiation. Single crystals were selected and mounted on a glass fiber at room temperature. All non-hydrogen atoms were refined with anisotropic thermal parameters. Hydrogen atoms were located at geometrically calculated positions and refined with isotropic thermal parameters. Table S1 show of crystallographic and refinement details, some selected bond distances and angles, and torsion angle are shown in Table S2. Table S3 display Hydrogen-bond geometry for compounds **1** and **2**.

Table S1. Experimental details for X-ray diffraction collected data and structural refinement.

	Compound 1	Compound 2
Crystal data		
Chemical formula	C ₁₁ H ₉ Zn _{0.50} Fe _{0.50} NO _{2.50}	C ₁₁ H ₉ Cu _{0.50} Fe _{0.50} NO _{2.50}
M_r	255.80	254.89
Crystal system, space group	Orthorhombic, <i>Pnna</i> (No. 62)	
Temperature (K)	100	173
a, b, c (Å)	11.7568 (9), 15.0687 (10), 11.1422 (7)	12.016 (2), 14.441 (2), 11.1347 (15)
V (Å ³)	1973.9 (2)	1932.1 (5)
Z	8	8
Radiation type	Cu $K\alpha$	Mo $K\alpha$
μ (mm ⁻¹)	7.73	1.89
Crystal size (mm)	0.06 × 0.06 × 0.14	0.05 × 0.14 × 0.16
Data collection		
Diffractometer	SuperNova, Dual, Cu at zero, Atlas	
Absorption correction	Multi-scan methodology.	
No. of measured, independent and observed [$I > 2\sigma(I)$] reflections	13774, 1988, 1765	11779, 2476, 1810
R_{int}	0.035	0.090
$(\sin \theta/\lambda)_{max}$ (Å ⁻¹)	0.623	0.703
Refinement		
$R[F^2 > 2\sigma(F^2)]$, $wR(F^2)$, S	0.028, 0.081, 1.06	0.047, 0.142, 1.07
No. of reflections	1988	2476
No. of parameters	147	147
No. of restraints	1	1
H-atom treatment	H atoms treated by a mixture of independent and constrained refinement	
$\Delta\rho_{max}$, $\Delta\rho_{min}$ (e Å ⁻³)	0.35, -0.60	0.90, -0.72

Computer programs: SHELXL2013 (Sheldrick, 2013).

Table S2. Selected bond distances, angles, and torsion angle for compounds **1** and **2**.

	Compound 1	Compound 2
Distances (Å)	M = Zn	M = Cu
M1—N1	2.084(2)	1.999(3)
M1—O2	2.145(1)	2.402(2)
M1—O1	2.164(1)	1.992(2)
N1—C1	1.337(2)	1.335(4)
N1—C5	1.344(2)	1.336(4)
C11—O1	1.265(2)	1.277(4)
C11—O2	1.272(2)	1.251(3)
Angles (°)		
N1—M1—N1 ⁱ	90.43(9)	89.7(2)
N1—M1—O2	99.86(5)	96.63(9)
N1 ⁱ —M1—O2	102.19(5)	101.80(8)
N1—M1—O1	93.88(5)	93.60(9)
N1—M1—O1 ⁱ	163.82(5)	161.27(9)
O2—M1—O1 ⁱ	94.47(4)	100.73(8)
O2—M1—O1	61.70(4)	59.51(8)
O2—M1—O2 ⁱ	148.49(7)	153.9(1)
O1—C11—O2	121.0(1)	121.9(3)
Torsion angle (°)		
C4—C3—C3 ⁱⁱ —C4 ⁱⁱ	-38.5(2)	-31.8(5)

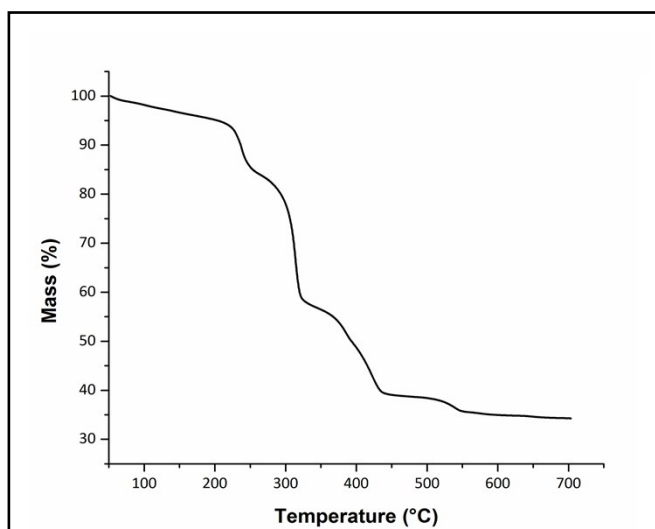
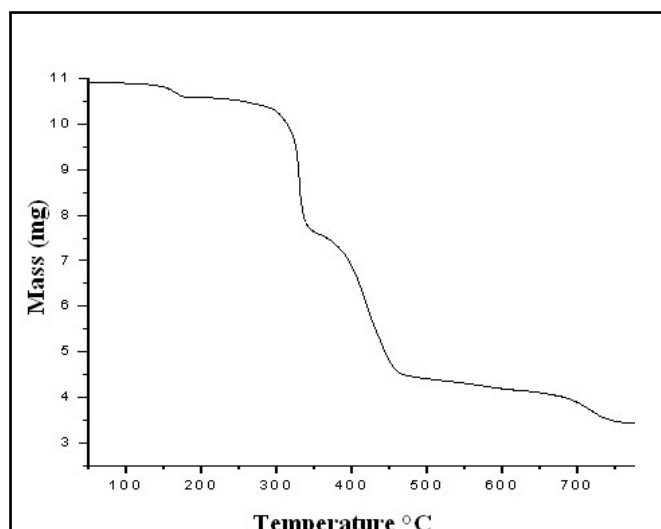
Symmetry codes: (i) $-x+3/2, -y+1, z$; (ii) $x, -y+1/2, -z-1/2$.

Table S3. Hydrogen-bond geometry (Å, °) for compounds **1** and **2**.

D—H...A	D—H/Å	H...A/Å	D...A/Å	D—H...A/°
Compound 1				
O1W—H1W...O1	0.90(2)	1.98(2)	2.867(2)	167(2)
C5—H5...O2	0.9500	2.5700	3.342(2)	139.00
C9—H9...O1W	1.0000	2.4400	3.322(2)	147.00
Compound 2				
O1W—H1W...O1	0.92(2)	1.99(2)	2.893(3)	167(4)
C5—H5...O2	0.95	2.39	3.084(4)	130.00
C9—H9...O1W	1.00	2.51	3.339(4)	141.00

7 TGA-Measurement.

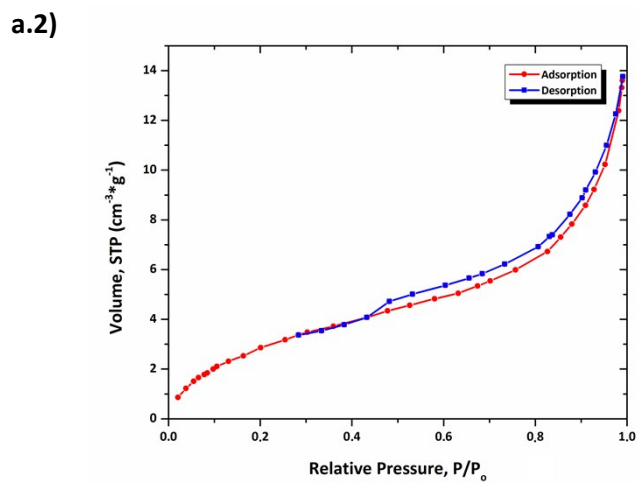
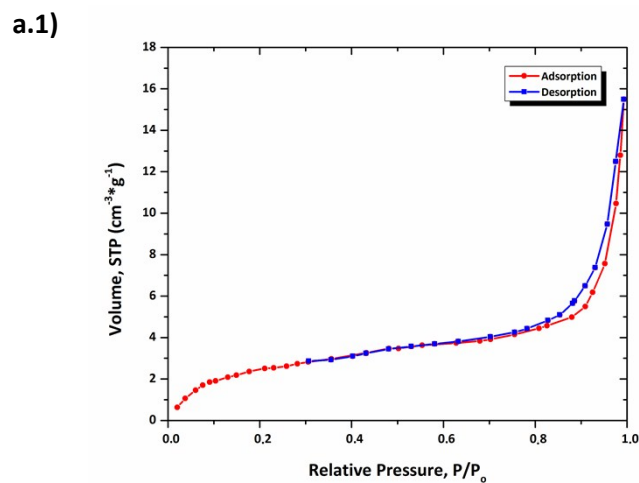
TGA measurements were performed on a Netzsch STA 409 PC by heating the sample from 50 to 600 °C at a rate of 10 °C min⁻¹ under nitrogen atmosphere.



(a) (b)
Fig. S5. TGA curves for compound **1** (a) and **2** (b), respectively.

8 N_2 gas Adsorption-desorption measurement.

The N_2 gas adsorption-desorption measurements were performed using a Micromeritics equipment, ASAP 2010. The N_2 sorption isotherms were collected in a relative pressure range from 0–0.97 at 77 K. The initial outgassing process for each sample was carried-out under vacuum at room temperature (291.15 K) for 8 h. Approximately, 50–60 mg of degassed samples were used for gas sorption studies. Total analysis times were ca. \approx 31 h. The purity of nitrogen gas was 5.0 ultrahigh purity grade. Pore properties including pore volume, pore size, and surface area were analyzed using ASAP2010 for Windows v3.02 software.



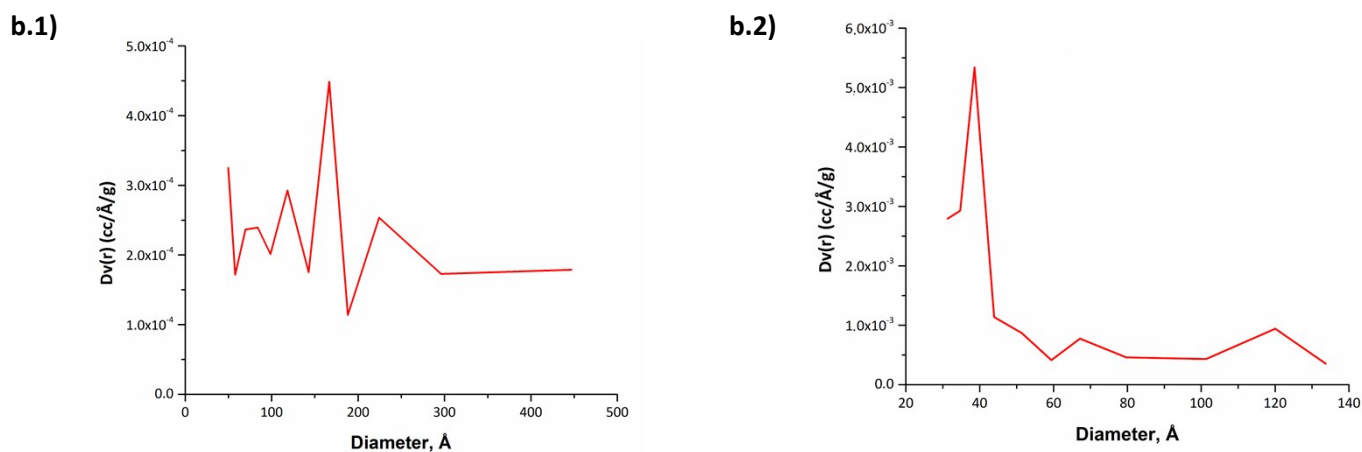


Fig. S6. Adsorption isotherms for N₂ (77 K). Red and blue line continued represent adsorption and desorption, respectively. (a) Represent adsorption isotherms saturation pressure (P_0) equals 760 Torr, N₂ at 77 K, for compounds **1** (a.1) and **2** (a.2). (b) Porous distribution for compounds **1** (b.1) and **2** (b.2).

9 Differential pulse voltammetry.

Differential pulse voltammetry studies were carried out on a Voltalab 80 (Radiometer Analytical) using a three-electrode configuration consisting of a Pt working electrode, a Pt auxiliary electrode, and a commercially available Ag/AgCl electrode as reference with a pure Ar gas inlet and outlet. The measurements were performed in DMF solution containing Tetrabutylammonium hexafluorophosphate (TBAPF₆) (0.1 M) as supporting electrolyte, with 50 ms pulses. The potential from +0.3 to +1.1 V was scanned at scan rate of 20 mVs⁻¹ and with 50 ms pulses.

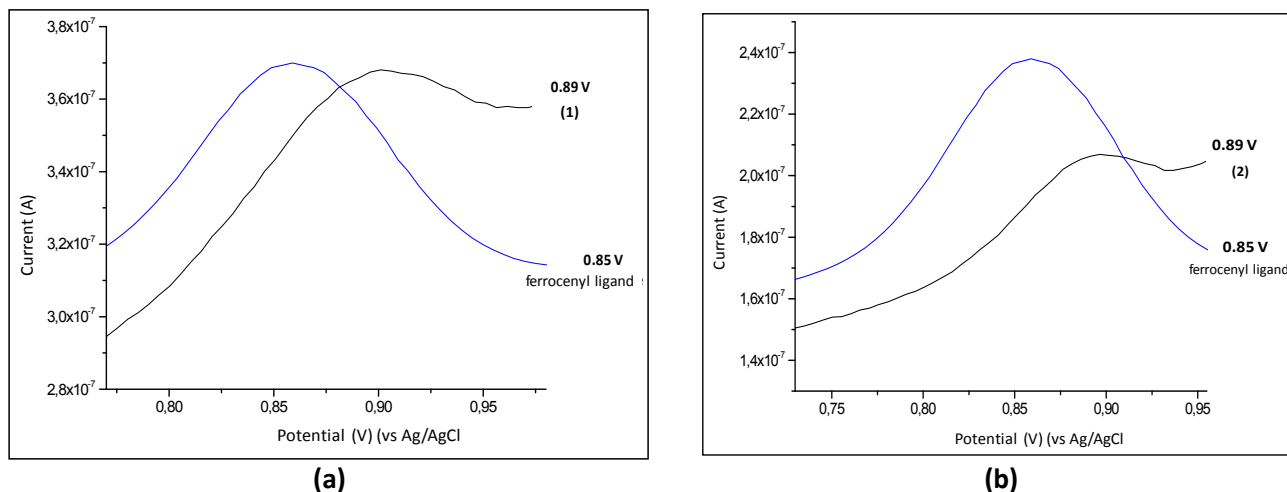


Fig. S7. Differential pulse voltammograms showing graphs for compounds **1**, **2** and 1,1'-ferrocenedicarboxylic acid, dissolved at a concentration of 1.0×10^{-3} M in DMF 0.1 M). The voltammograms were carried out at a scanning rate of 20 mVs⁻¹ (vs. Ag/AgCl).